Institute for Laser Physics of SC "Vavilov State Optical Institute"
& Lasers and Optical System, Ltd.

Optically Addressed Spatial Light Modulator Development For Compensated Imaging By Real-Time Holography

SPC 98-4062
Contract F61775-98-WE098

FINAL REPORT

Director of the Institute — **Prof. Arthur A. Mak**

Principal Investigator — **Vladimir A. Berenberg**

St.-Petersburg
1999

REPORT DOCUMENTATION PAGE

Form Approved OMB No. 0704-0188

1. AGENCY USE ONLY (Leave blank)	2. REPORT DATE	3. REPORT TYPE AND DATES COVERED
	1999	Final Report

4. TITLE AND SUBTITLE

Optically Addressed Spatial Light Modulator Development for Compensated Imaging by Real-Time Holography

5. FUNDING NUMBERS

F61775-98-WE098

6. AUTHOR(S)

Dr. Vladimir A. Berenberg

7. PERFORMING ORGANIZATION NAME(S) AND ADDRESS(ES)

Lasers and Optical Systems
14 Birzhevaya line
St. Petersburg 199034
Russia

8. PERFORMING ORGANIZATION REPORT NUMBER

N/A

9. SPONSORING/MONITORING AGENCY NAME(S) AND ADDRESS(ES)

EOARD
PSC 802 BOX 14
FPO 09499-0200

10. SPONSORING/MONITORING AGENCY REPORT NUMBER

SPC 98-4062

11. SUPPLEMENTARY NOTES

12a. DISTRIBUTION/AVAILABILITY STATEMENT

Approved for public release; distribution is unlimited.

12b. DISTRIBUTION CODE

A

13. ABSTRACT (Maximum 200 words)

This report results from a contract tasking Lasers and Optical Systems as follows: The contractor will investigate and develop improved techniques for producing superior performance optically addressed, spatial light modulators for research use in adaptive optical systems and deliver six such devices for AFRL research use.

14. SUBJECT TERMS

EOARD, Adaptive Optics, Liquid Crystals, Image Processing, Holographic Devices, Ferroelectrics, Deep space imaging, Optically addressed spatial light modulators

15. NUMBER OF PAGES

21

16. PRICE CODE

N/A

17. SECURITY CLASSIFICATION OF REPORT	18. SECURITY CLASSIFICATION OF THIS PAGE	19. SECURITY CLASSIFICATION OF ABSTRACT	20. LIMITATION OF ABSTRACT
UNCLASSIFIED	UNCLASSIFIED	UNCLASSIFIED	UL

1. Introduction

This document is the Final Report on the Contract # SPS-98-4062 with EOARD. The results are described of the development of technology for deposition blocking layers and high-reflective dielectric mirrors operating in visible onto thin photosensitive a-Si:C:H layers. Five samples of optically-addressed spatial light modulators (OA SLMs) are manufactured and tested, with various types of dielectric mirrors, both with and without blocking layers. The characteristics of these samples are studied and described.

2. Development of an optically addressed LC SLM with dielectric mirror and light-blocking layer

2.1. Multilayer mirrors based on amorphous hydrogenated silicon carbide (a-Si:C:H) films

Basic requirements to multilayer mirrors for OA SLM

1. Mirrors should provide the reflectance close to 100% and, consequently, a low transmition for the readout light. However, it should be noted that the reflectance of 60-90% is sufficient for most of applications, and the main requirements are imposed on the low transmittance of a multilayer mirror (MLM). This implies that the use of absorbing layers in such MLMs is allowable provided that this will not cause heating of an SLM as a whole.
2. The conductivity of the MLM layers should be matched to that of a liquid crystal. In an ideal case, an MLM should show such a transverse conductivity that the voltage drop across the MLM be minimum and, at the same time, show a minimum longitudinal conductivity so that to prevent spreading the charge over the MLM layers.
3. The capacitance of an MLM should be maximum, hence, the thickness be minimum. In this case, the voltage drop across an MLM will be minimum if pulsed voltage is applied to the mirror.
4. The MLM layers and interfaces in-between them should not contain a large number of deep centres or charge-carrier adhering traps to avoid the image memory effect.
5. The MLM layer deposition technology should be consistent with the technology for preparation of other MLM layers.

2.2. Material and MLM layer preparation technique options

We have chosen amorphous hydrogenated silicon carbide layers, produced by the plasma chemical vapor deposition (PECVD) technique, as a material for the MLM. The MLM layers were prepared using the same technique as that used for the production of the photosensitive layer in a common technological process. In addition to its technological compatibility with the process of the photosensitive layer fabrication, among the advantages of this MLM production technological process is the possibility to vary optical and electrical parameters of the a-Si:C:H layers within a wide range by altering the composition of a gas mixture used in the film deposition process.

The a-Si:C:H layers were deposited on a substrate, its temperature being 200-250 C, the working gas mixture pressure being 0.1-0.3 torr, and the frequency of a RF generator being 17 MHz. We used a silane-methane-argon mixture. Fig. 1 shows conductivity σ and refractive index n of the a-Si:C:H films produced vs. the methane-silane ratio in the gas mixture. The conductivity and refractive index decrease as the methane content increases in the gas mixture. It is seen from the figure that refractive index n varies from 4 to 1.8-1.6. Such a wide n variation range makes it possible to fabricate a smaller number of the MLM layers to attain the

assigned optical characteristics and makes the use of such layers very promising for the MLMs.

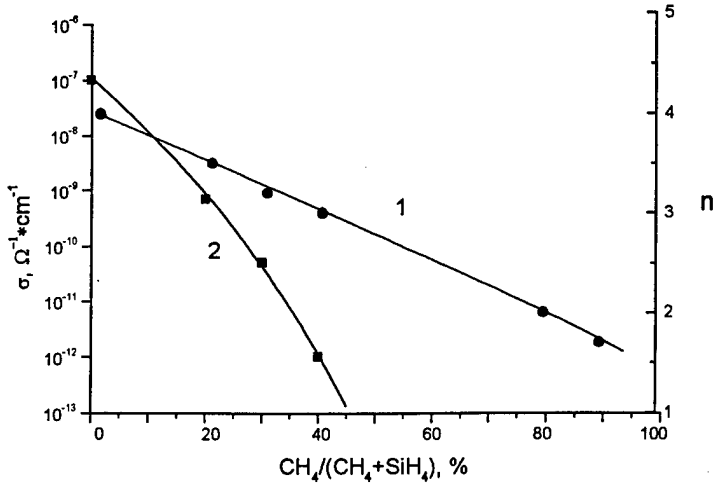

Fig.1. Refractive index (1) and conductivity (2) vs. the methane content in the gas mixture.

2.3. Calculation of optical characteristics of an MLM with a-Si:C:H layers

To choose the optimal design of an MLM and to match its electrical and optical characteristics to the parameters of other layers in an SLM, we calculated the optical characteristics of the MLM as a function of optical characteristics of individual a-Si:C:H films, the variation in *n* and absorption coefficient with altering the gas mixture composition being taken into account. The films with smaller refractive index accordingly showed smaller absorption coefficient in the visible spectral range.

Fig. 2 depicts the calculated transmission spectrum and the spectral dependence of 1-R, R being the reflectance, for a seven-layer mirror, the layer thickness' and reflective indices respectively being $n_1 = 3.2$, $d_1 = 40$ nm and $n_2 = 1.8$, $d_2 = 80$ nm. These parameters were chosen as being most realistic for implementation of the technique of the a-Si:C:H layer deposition in the common technological cycle. Note that it is possible to use a layer with the larger *n*, however, in this case, its conductivity will be larger than the dark conductivity of the a-Si:C:H photosensitive layer, which may result in the image blurring. As can be seen from this figure, the absorption in the a-Si:C:H layers becomes to be exhibited in the spectral range with wavelengths shorter than 0.6 μm. Our calculations demonstrate that the absorption can be lower than 10-20% at a wavelength of 0.5 μm. Hence the mirrors thus produced will show the required reflectance (>80%) in a wavelength range shorter than 0.5 μm. The position of the minimum depends on the layer thickness and it can be interferometrically monitored during the deposition process. The transmission in the minimum of the spectral dependence is a function of the optical parameters of the layers, their thickness and number.

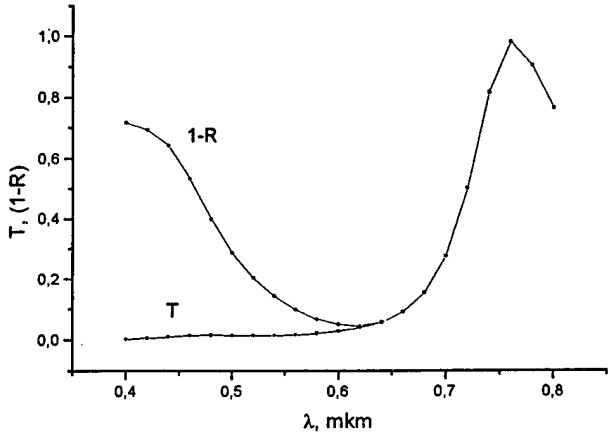

Fig.2. Calculated spectral dependencies of transmittance T and 1-R, R being the reflectance, for a seven-layer structure.

Thus, theoretical calculations demonstrate that it is possible to fabricate multilayer mirrors with a-Si:C:H layers whose conductivity is lower than or is on the order of magnitude of the dark conductivity of a photosensitive layer, the layer thickness being less than 0.5 μm, the reflectance being higher than 80% in the wavelength range shorter than 0.5 μm, and the transmittance being lower than 5% in the minimum of the spectral dependence.

2.4. Experimental results

Prior to depositing the a-Si:C:H layers on an MLM, we preliminary prepared the layers with the methane content in the gas mixture being varied. Their characteristics are listed in Table 1. Layer # 618 showed a high conductivity and could not be used for fabrication of the MLM. The rate of deposition of layer # 621 was two-three times lower as that of layer # 620; therefore, a pair of layers # 619 and 620 was chosen for the reasons of technological nature.

Table 1.

Sample	$\%CH_4/\Sigma$	σ_d, $\Omega^{-1}cm^{-1}$	σ_{ph}, $\Omega^{-1}cm^{-1}$	*d*, nm	*n*
618	0	10^{-7}	10^{-5}	40	4.0
619	30	$5x10^{-11}$	10^{-9}	45	3.2
620	80	$<10^{-12}$	$<10^{-12}$	80	2.0
621	90	$>10^{-12}$	$<10^{-12}$	90	1.7

Fig. 3 shows the transmittance T and 1-R of an MLM vs. the number of layers, N_S, for λ_{min} = 0.63 μm. As one can see from this figure, the transmittance being lower than 5% in the minimum can be obtained in a structure containing 7 layers.

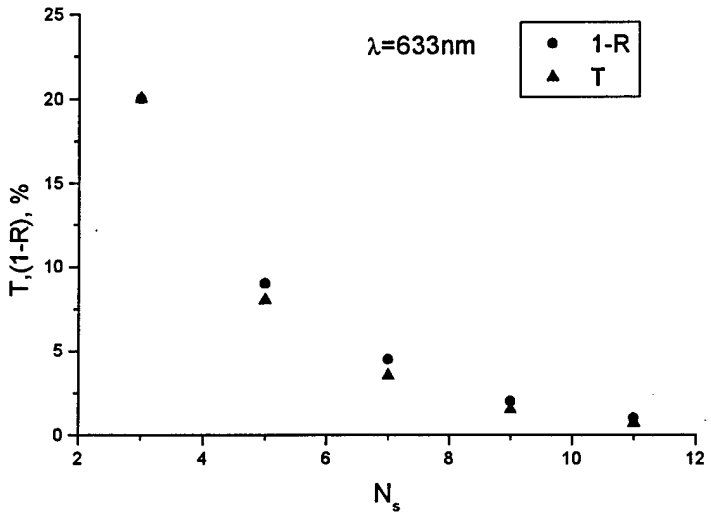

Fig.3. Transmittance T and 1-R at the minimum in the spectral dependence vs. the number of layers in a multilayer structure.

Fig. 4 depicts the transmittance in the minimum of the spectral dependence vs. the refractive index of a layer with small *n*. To obtain a transmittance lower than 5% in a seven-layer structure, it is necessary to produce a-Si:C:H layers with *n* smaller than 2.0.

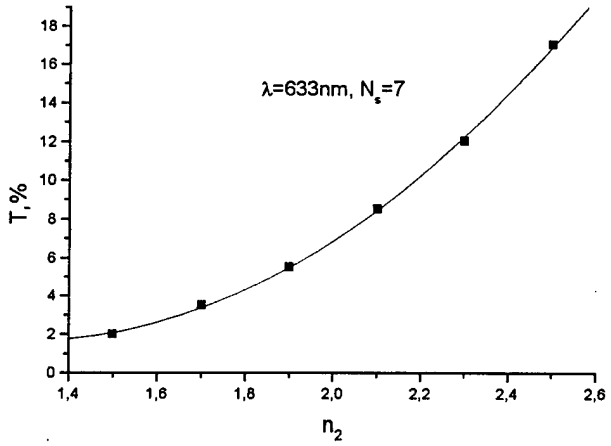

Fig.4. Transmittance at the minimum of the spectral characteristic of a seven-layer structure vs. the refractive index of an a-Si:C:H layer with a broad energy band.

Using these structures, we have fabricated the mirrors with various number of the layers, namely, three, five, and seven. The mirrors with three and five layers were made to provide the minimum transmission at a wavelength of about 630 nm, and the seven-layer mirror at about 530 nm. The reflection spectra of these MLMs are shown in Fig. 5. As can be seen, the reflectance at the maximum is about 60% for the three-layer mirror and 90% for the five- and

seven-layer mirrors. According to the theory, as the number of layers increases, the spectral region with high reflectance R narrows. Note that the reflectance's of the five- and seven-layer mirrors are almost the same, because the latter one was fabricated to provide the maximum reflectance at 530 nm. In this spectral region, the absorption becomes significant and amounts to about 10%, which hinders the increase in reflectance as the number of layers increases to seven.

For a comparison, curves 4 and 5 in Fig. 5 accordingly depict the spectral dependencies of the reflectance of pixelated Al mirrors with 30- and 5-μm pixel size, the interpixel spacings being 2 and 1 μm, respectively. The low values of reflectance R of the mirror with the small-size pixels is apparently attributed to the low-quality lithography, which caused strong scattering form the Al layer.

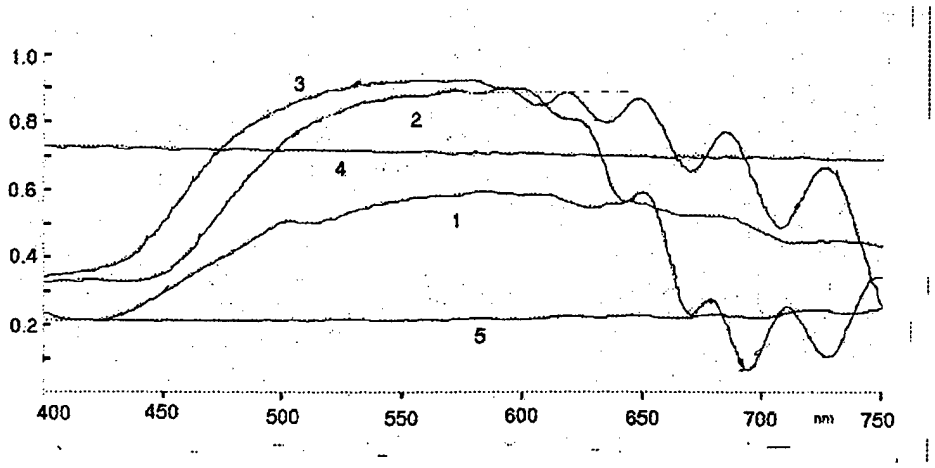

Fig.5. Reflection spectra of multilayer mirrors. Curves 1, 2, and 3 respectively correspond to a three, five-, and seven-layer mirror. Curves 4 and 5 correspond to Al mirrors with 30- and 5-μm pixels spaced at 2 and 1 μm, respectively.

3. Investigation of photoconductor/ light-blocking layer/dielectric mirror structures for OA SLMs

Our study showed that a problem of optical decoupling between the write and read light beams can not be decided by a dielectric mirror (DM), which is placed between the FLC's and a photoconductor of the OA SLMs. DM cannot really provide total reflection of the read light in OA SLMs operating in reflection mode. The visible light field, which penetrates into the photoconductor layer adjacent to the mirror, is absorbed therein, thus affecting the light modulation. The more effective isolation of write and read light fluxes can be placing of a read-light-absorbing layer between the mirror and the photoconductor. We have found that an amorphous hydrogenated carbon (a-C:H) film absorbing light in the visible region of spectrum can use as light-blocking layer (LBL) for optical isolating a-Si:H and a-Si:C:H photoconductor, utilized in OA SLM's. The a-C:H LBL was deposited on top of the photoconductor at the ambient temperature from acetylene by PECVD process using a glow discharge on dc. It is a new technological solution of the problem of optical decoupling between the write and read light beams in OASLMs. We study here the optical and electrical properties of LBL to optimize the performance characteristics of an reflective type FLC OA SLM with DM.

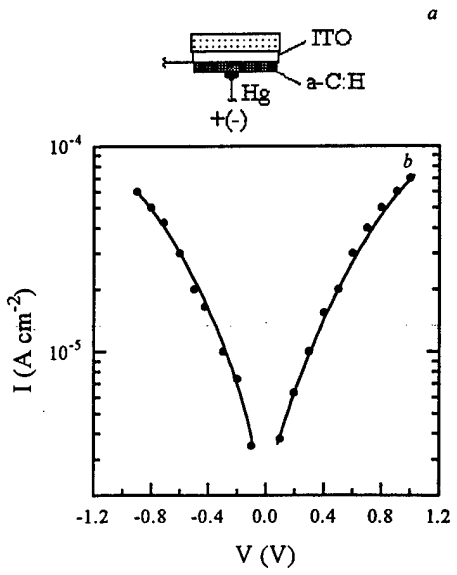

Fig.6. Schematic diagram of a measurement setup (*a*) and the I-V characteristic (b) of the current density *I* vs. positive and negative voltages *V* for an ITO/a-C:H/Hg-contact structure ($\rho = 2\times10^{9}$ Ωcm).

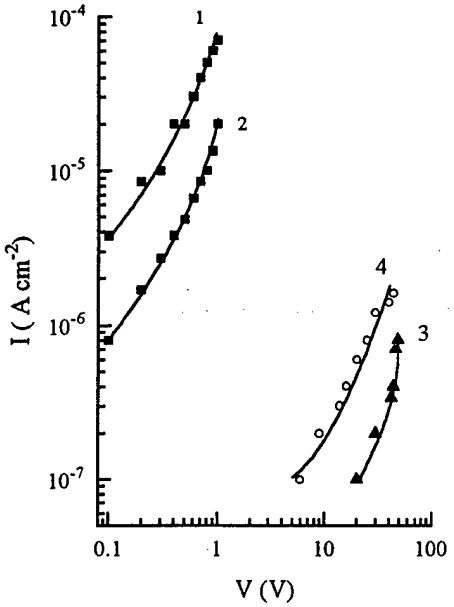

Fig.7. Dark I-V characteristics for ITO/a-C:H/Hg-contact structures, a-C:H films being produced from an acetylene plasma under various conditions.

To determine resistivity ρ of LBL, we deposited 0.1-0.3 μm thick a-C:H films on the surface of a transparent conductive electrode made from indium-tin oxides (ITO) deposited on glass substrates using laser sputtering. When measuring current density *I* as a function of voltage *V* applied, the ITO layer and a mercury droplet were respectively used as a bottom and metal contacts (see Fig. 6a), the area of the Hg-contact being ~0.01 cm^{2}. For the ITO/a-C:H/Hg-contact structures, the I-V characteristics were symmetric when the resistivity of the a-C:H films lay within the $7\text{x}10^{8}$-$1\text{x}10^{12}$ Ωcm range [1]. Fig. 6b depicts a dark I-V characteristic for an a-C:H layer with $\rho = 2\times10^{9}$ Ωcm. The symmetry in the I-V characteristics, negative and positive voltages being applied, has been observed in Ref. 2 for metal/a-C:H/metal structures with the upper contacts made from Al and Cr. The symmetric I-V characteristic is evidence that the current is independent of the electronegativity of the contact and is governed by the electronic structure of the a-C:H film. At the same time, the conductivity of a-C:H films is specified by the optical band gap. It is typical for a-C:H that the traps deepen as the optical band gap widens, the latter being much narrower than the former.

Fig. shows the dark I-V characteristics for ITO/a-C:H/Hg-contact structures, which were obtained when a positive voltage was applied across a-C:H films produced under various conditions. Curves 1 and 2 correspond to films with the optical band gap $E_T \le 1$ eV, low resistivity ($\rho < 10^{9}$ Ωcm), and with an activation energy of the conduction process of several tenths of electron-volt. Curves 3 and 4 in Fig. 7 are typical for an a-C:H modification with $E_T \ge 1.5$ eV and $\rho > 10^{10}$ Ωcm. Fig. 8 shows a spectral dependencies of the transmittance of the a-Si:C:H/LBL structures in the 400-1000-nm spectral range. The transmittance is $T < 0.03\%$ at $\lambda = 400$-550 nm within the limits of measurement accuracy. The a-C:H LBL

with thick of 0.3-0.5 μm can really isolate green light with a wavelength of 550 nm.

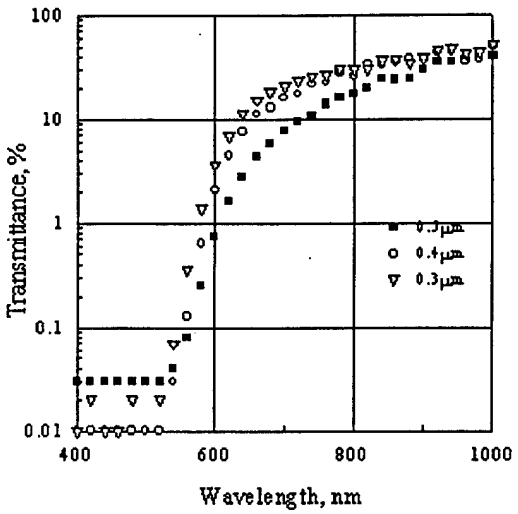

Fig.8. Transmittance of an a-Si:C:H/LBL structure, the LBL thick were 0.3-0.5 μm.

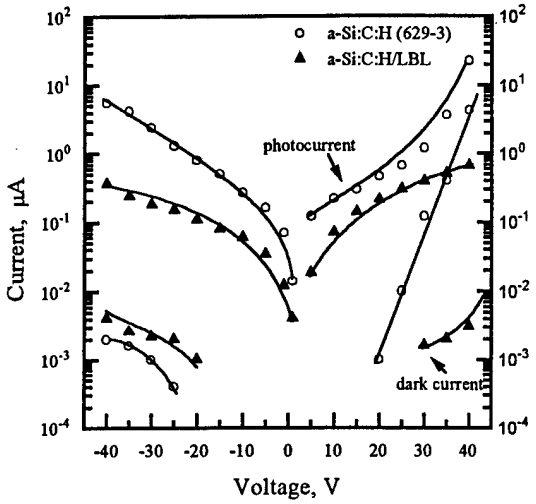

Fig.9. Dark and photocurrent *I* vs positive and negative voltages *V* for ITO/a-Si:C:H and ITO/a-Si:C:H/LBL structures.

Fig.9 shows the current density *I* vs. voltage *V* applied for ITO/a-Si:C:H and ITO/a-Si:C:H/LBL structures. Similar to the schematic diagram in Fig.6a, here we used a mercury droplet as a metal contact to measure the I-V characteristics. As voltage increased in the intrinsic a-Si:C:H layer, an exponential dark current increase was observed in the direct directions. Under these conditions, the ITO/a-Si:C:H/Hg-contact structure shows a low resistance. The dark I-V characteristic of the ITO/a-Si:C:H/LBL structure is different from those of the photosemiconductor. One can see that the curves for the direct and reverse currents in the ITO/a-Si:C:H/LBL structure are symmetric, and the current increases as resistivity ρ of the a-C:H layer decreases. Such a behavior of the I-V characteristics for the positive and negative voltages applied was observed for the metal/a-C:H/metal structures as well. As voltage increases, the resistance of the films grows, and the voltage dependence of current departs from the Ohm law. The non-ohmic behavior of the resistance of a-C:H films produced by the chemical vapor deposition in plasma was earlier noticed in Ref. 3.

The photocurrent depends not only on the photosensitivity of a-Si:C:H, but also on the electronic structure and conductivity of the a-C:H LBL. Charge carriers, being photo-induced in a-Si:C:H, pass through the a-C:H layer unimpeded, or they are trapped in the band of the high-density localized states of LBL. The conductivity of a-C:H being governed by the carrier trapping in this band [4]. To attain an efficient light isolation, it is expedient to use an absorbing a-C:H layer with an optical band gap of ~ 1 eV and resistivity ρ falling within the 10^{10}-10^{11} Ωcm range.

The current-voltage characteristics of the a-Si:C:H /LBL/DM structures, when DM was deposited on top of the LBL, are shown in Fig. 10 and 11. They differ from the I-V dependencies of a-Si:C:H /LBL essentially. 5 layers mirror based on a-Si:C:H (Fig.10) has a high resistance and decreases the photocurrent pass through the a-Si:C:H /LBL on two orders within interval voltage 10-40 V in the result of trapping charge carriers. OA SLM assembled with that multilayers structure will be work effectively under high positive voltage. Deterioration of I-V characteristics of the a-Si:C:H /LBL was observed in the case of using 11

layers mirror based on HfO_2 and SiO_2 (Fig.11).

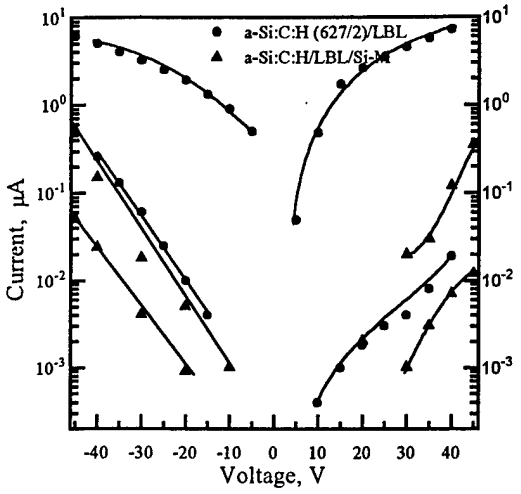

Fig.10. Dark and photocurrent I vs positive and negative voltages V for ITO/a-Si:C:H/LBL and ITO/a-Si:C:H/LBL/Si-mirror structures.

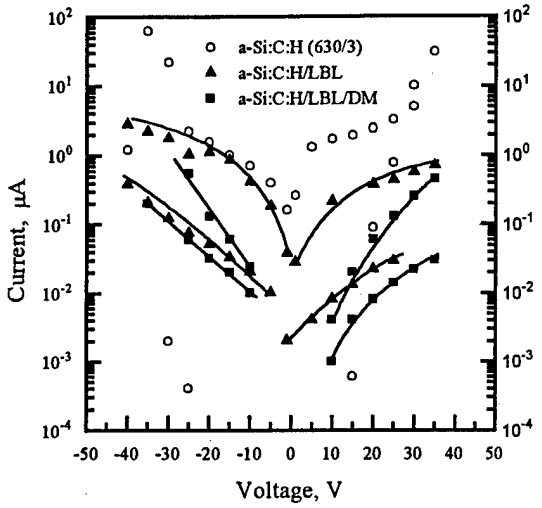

Fig.11. Dark and photocurrent I vs positive and negative voltages V for ITO/a-Si:C:H, ITO/a-Si:C:H/LBL and ITO/a-Si:C:H/LBL/DM structures.

4. Studies of OA SLM Characteristics with Blocking Layers and Dielectric Mirrors.

Several samples of OS SLMs were manufactured varying in design, The influence of blocking layer and dielectric mirrors to SLM characteristics were studied. Two samples (D1 and D2) had no blocking layer, and differed in dielectric mirror design. The sample D1 had the mirror consisting of 11 quarterwave layers of Hafnium and Silicon oxides, the reflection coefficient of the mirror equals to ~ 74% at λ=0.53 micron. The sample D2 had the mirror consisting of 5 quarterwave layers of Silicon and ITO/a-Si:C:H, the reflection coefficient of the mirror equals to ~ 80% at λ=0.53 micron. The ferroelectric LC operating with the Clark-Lagerwall effect was used with these samples. The characteristics of LC layer: tilt angle of LC director 22.5°, LC thickness ~5 micron. The sample D3 differs from D2 by the presence of the blocking layer, and the other type of ferroelectric LC was used operating with DHF effect, tilt angle of LC director was ~ 40^0. The characteristics of SLMs studied are given in the table 2.

The measurements of diffraction efficiency (DE) at various spatial frequencies under the variation of write radiation intensity, repetition rate F and peak-to-peak amplitude of driving voltage V_{pp}, bias voltage V_b, and orientation of holographic grating vector and read-out radiation polarisation to the normal to smectic layers. The value of DE was defined as the ratio of the maximal (in time) intensity of read-out radiation reflected in the first diffraction order to the corresponding value of the reflected from SLM radiation in the absence of the holographic grating.

Table 2.

Photoconductor	Light block layer	Mirror	FLC	SLM
a-Si:C:H (616)	-	11 λ/4 HfO_2,SiO_2	SSFLC (22,5^0), ~5 μm	D1
a-Si:C:H (623)	-	5 λ/4 Si	SSFLC (22,5^0), ~5 μm	D2
a-Si:C:H (629/3)	a-C:H, ~ 0.5 μm	5 λ/4 Si	DHF (40^0), ~5 μm	D3

The He-Ne laser, λ=0.63 micron, was used to write in the holographic grating. The CW laser radiation was modulated by Π-shaped pulses, with pulse duration and repetition rates synchronized with the electrical pulses driving the SLM. The writing beams had equal intensity, and their diameter in the plane of photoconductor (PC) equaled to 8 mm. The read-out was done by CW plane-polarized radiation either of He-Ne laser, λ=0.63 micron, or solid-state laser (λ=0.53 micron). When the DE of SLM without LBL was studied, the intensity of the read-out laser radiation was reduced to the level not affecting the value of DE. For the SLMs with LBL the influence of the reading radiation to DE was absent for all range of read-out intensity (the maximal density of read-out radiation was ~ 800 μW/cm^2).

The main results of these studies are as follows:

- The dependence of DE for the samples D1, D2 and D3 is substantially different for various conditions of the holographic grating writing.
- For the SLM D1, the maximal value of DE was 7.3% at the holographic grating spatial frequency 28 lp/mm, with the values of driving voltage V_{pp} = 25 V, biais voltage V_b = 22 V, and repetition rate F = 10 Hz (the time duration of the driving and illuminating pulses equal to 50 ms). With the decrease of the repetition rate F down to 1 Hz, the DE smoothly decrease to the value 5-6%. With the F increase, starting from F=60-70 Hz, the dramatic (5-10 times) drop of DE was observed.
- For the SLM D2 the maximal value of DE was 21% at the holographic grating spatial frequency 28 lp/mm, with the values of driving voltage V_{pp} = 30 V, biais voltage V_b=0 V, and repetition rate F = 33 Hz. With the F increase, the DE efficiency drop was also observed, but less expressed than that for SLM D1. For F=100 Hz, the maximal value DE=13.9%. It was noticed that the diffraction response appeared not during the write-in time, as it was for SLM without mirrors, but during the erasing time, when the writing radiation did not exist. Probably, this is the evidence of a substantial influence of the mirror to the balance of driving voltage between photoconductor and FLC layers. The significant (7 times) variation of DE with the angle of the read-out light polarization to the normal of smectic layers from 0^0 to 90^0 was observed.
- For the SLM D3, the dependence of DE on the repetition rate F was monotonous, but the DE value at various repetition rates was of the same order as for the SLM D2. The value of DE for F<10 Hz equals to ~25% (λ=0.63 micron) for the spatial frequency 28 lp/mm. With the repetition rate F increasing, the DE value decreases, and for F=100 Hz DE=12.3%, under V_{pp} = 50 V and V_b = 24 V. At the same time, we shall notice that these DE values were obtained under the write-in radiation density lower than the optimal value. This is connected with the lower sensitivity of the SLM D3, and the corresponding increase of write-in radiation density was above the opportunities of our equipment. Unlike the SLM D2, the response appeared during the write-in cycle, and it existed until the moment of driving voltage switching. Thus, the dynamics of FLC orientation does not differ qualitatively from that for SLM without mirror. Seemingly, this can be explained by the better matching of electrical layers impedance, as compared to the SLM D2. The SLM D3 exhibits only negligible dependence of DE

on the orientation of read-out light polarization to the normal to smectic layers. For the changing wavelength of read-out radiation (λ=0.53 micron), for the same values of V_{pp} and V_b, the value of DE decreased approximately to 1.6 times. But, for the driving voltages rise to V_{pp} = 60 V and V_b = 30 V, DE restored to the previous values.

- For all three samples SLM, the significant DE drop was observed for spatial frequencies >40 lp/mm. This effect can be connected with poor matching of electrical impedance of mirrors and blocking layers with PC and LC layers.

The Figs.12-15 give the illustration the said above. In the Figs.12-15, the dependence of DE vs write-in radiation intensity for SLM D2 and D3, the angle between normal to smectic layers and the polarization of read-out radiation and the spatial frequency of grating being as parameters. The curves of the Figs.12-14 were obtained for the spatial frequency of grating 28 lp/mm; the curves on Figs. 12, 14 and 16 were measured for F=100 Hz. For all the cases, the duration of write-in pulses and driving voltage pulses were equal to ½ of driving pulses time period T=1/F.

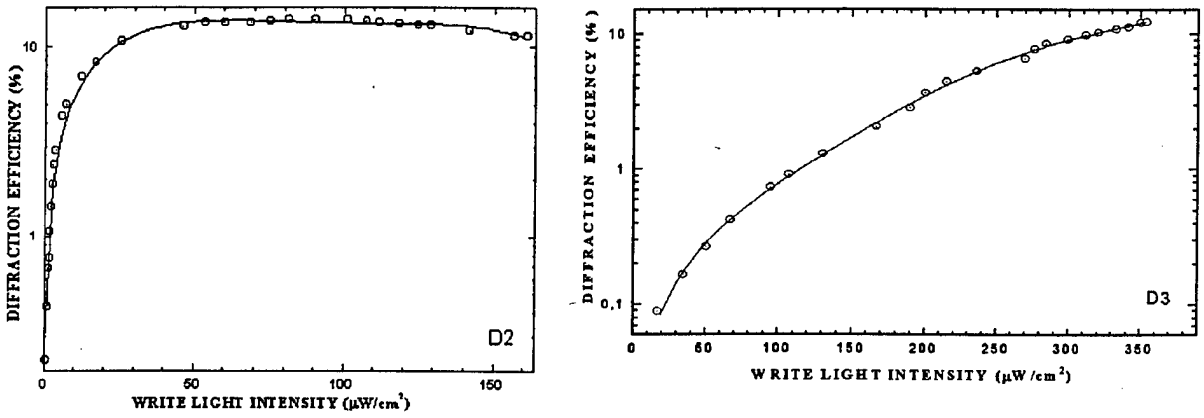

Fig.12. Diffraction efficiency DE vs write-in light intensity.

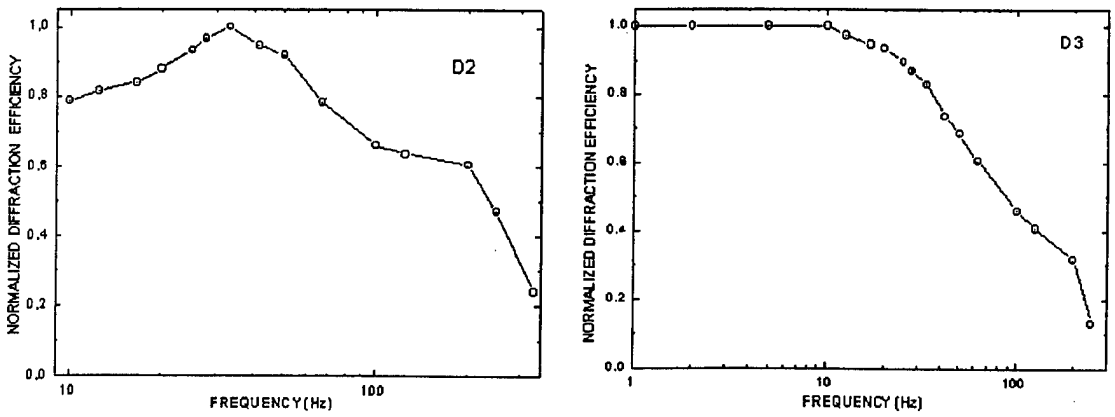

Fig.13. Diffraction efficiency DE vs driving voltage repetition rate.

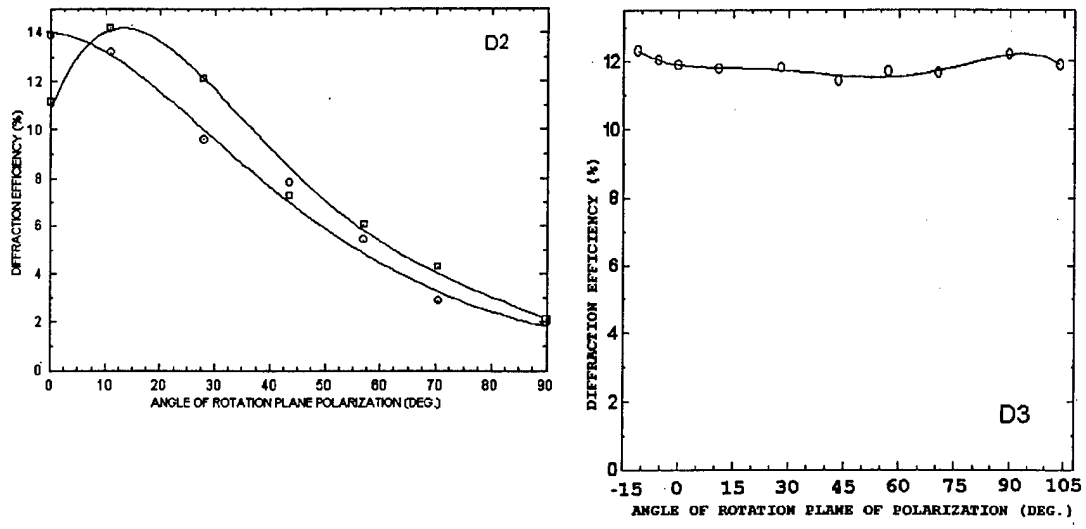

Fig.14. Diffraction efficiency DE vs the angle between read-out polarization and the normal to the smectic layers. For the SLM D2, the cases of the grating vector parallel and orthogonal to the normal to smectic layers are shown.

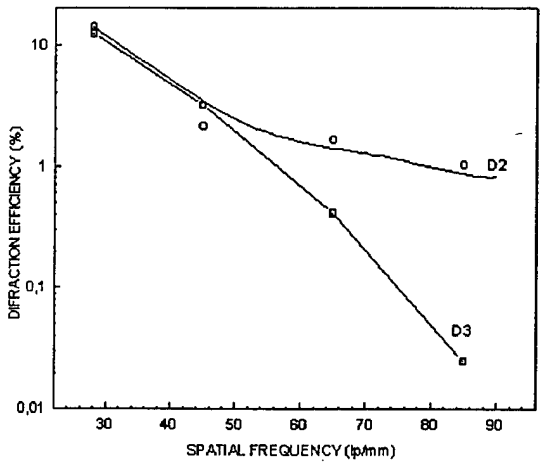

Fig.15. Diffraction efficiency DE vs the grating spatial frequency.

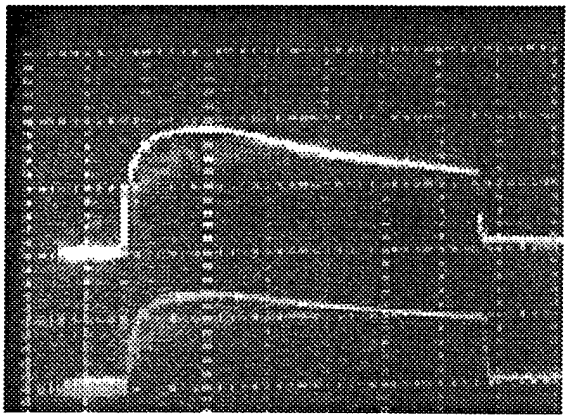

Fig.16. Diffraction efficiency DE vs time for SLM without mirror, for the read-out by two orthogonally-polarised beams with equal intensity. Time scale 0.5 s.

One of the most important requirements for OA SLM as optical correctors for observational telescopic systems is that of low DE dependence on the polarization direction of the reading light, because the observation of objects is made, generally, in the non-polarized light. As it is evident from the results presented, this dependence may be quite different depending on which effect is used, Clark-Lagerwall or DHF. The fact that the character of the polarization dependence of DE is determined mainly by the type of the electrooptic effect used for the hologram writing, is confirmed by the results of measurements of DE for OA SLM containing various PC layers. As the illustration, the Fig.16 represents an oscillograms of DE variation vs time for an SLM with polymer PC under reading by two orthogonally-polarized beams of He-Ne laser, the angle between beams being ~ 0.04 rad. The writing of the grating at

SLM was done by pulses of light with the wavelength λ=0.53 μm with time duration τ=20-30 ns at the repetition rate F = 1/6 Hz and the spatial frequency 100 lp/mm. For these conditions, the maximal value of DE was equal to 18%.

An explanation of a possible cause of the various DE behavior on the light polarization direction depending on the electrooptic effect used is given below.

5. Theoretical study of orientation dependence of DE for holographic correctors written using Clark-Lagerwall and DHF effects.

5.1 Main relations using for DE orientation dependence evaluation.

For FLC SLM, the mutual arrangement of smectic layers, LC director n, and the vector of polarization Pc normal to n, is shown in Fig.17a. Under the electrical field E applied, a moment of force arises, which tends to re-orient the LC director into equilibrium position (PC||E), rotating it along the generatrix of the cone with the vertex angle 2θ and axis X coincided with the normal to smectic layers which are perpendicular to SLM substrates [5]. While writing-in the diffraction grating, the components of electric fields are forming inside the bulk of LC both parallel and perpendicular to SLM substrates. Therefore the gratings with the different orientation of the vector of grating are not equivalent a priori. The manifestation of this non-equivalence, as it is evident from the experiments, is dependent significantly on the characteristics of LC, blocking layers, mirror, and on the character of interaction between FLC and its bounding surfaces. It is difficult now to make more instructive statements basing on the data obtained. It is necessary to build a theory of the process of formation of diffraction grating in optically addressed FLC SLMs, which is meets, essential difficulties.

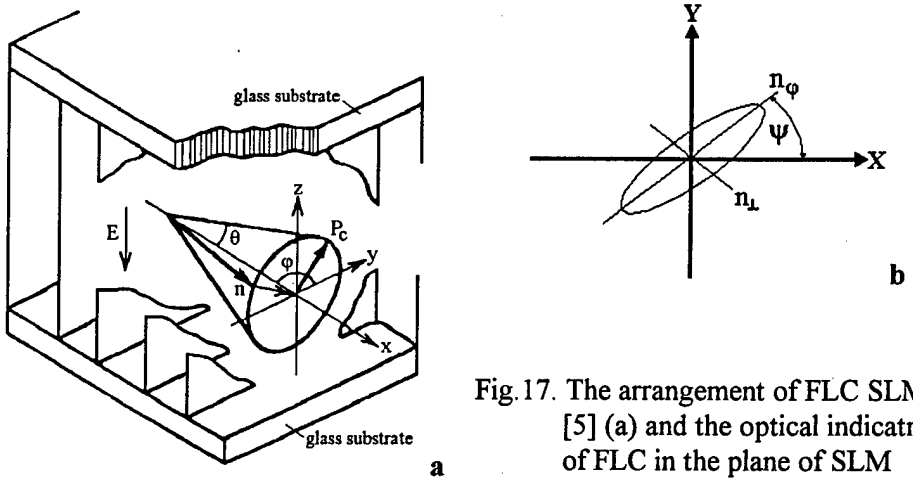

Fig.17. The arrangement of FLC SLM [5] (a) and the optical indicatrix of FLC in the plane of SLM substrate (b).

At the same time, a qualitative dependence of DE of the direction of the linear polarization of reading light can be analyzed relatively simply. The reason is that, for the reading radiation, the complex movement of the optical indicatrix is reduced to its tilting in the plane of blanks about the axis X to a certain angle ψ that is a function of the azimuthal angle φ, and to variation of extraordinary refraction index n_φ (Fig.17b). If the reading radiation enters SLM normally, the following formulae can be written for the angles ψ and n_φ [6]:

$$\mathrm{tg}\psi = \mathrm{tg}\theta\cos\varphi, \qquad n_\varphi = n_\perp\left[g^2 + \left(1-g^2\right)\sin^2\theta\sin^2\varphi\right]^{-1/2}, \tag{1}$$

here $g = n_\perp/n_\parallel$, $n_\parallel$ and $n_\perp$ is the main values of the refractive index.

In order to calculate DE, it is necessary to find the matrix T linking the reading field intensity at the input and the output of SLM:

$$\begin{pmatrix} E_X^{out} \\ E_Y^{out} \end{pmatrix} = T^* \begin{pmatrix} E_X^{in} \\ E_Y^{in} \end{pmatrix}. \tag{2}$$

By assigning various functional dependence of the angle φ of the coordinate along the vector of grating, one can reveal qualitatively peculiarities of behavior of DE depending of the polarization of reading radiation, FLC characteristics, and the type of the electrooptic effect used.

According our assessments, the character of propagation of a plane wave remains rectilinear as it travels, under small angles, through a modulated layer of LC with thickness h while $h/\Lambda \le 1$ (Λ is the period of the holographic grating). In these conditions, only the phase of wave changes. Then, assuming $\varphi = \text{const}$ along the wave path and using the optical path presentation, the matrix T can be represented as:

$$T = \begin{pmatrix} A & B \\ B & C \end{pmatrix}, \tag{3}$$

where $A = \exp(ikn_\varphi h)\cos^2\psi + \exp(ikn_\perp h)\sin^2\psi$, $\quad C = \exp(ikn_\varphi h)\sin^2\psi + \exp(ikn_\perp h)\cos^2\psi$,

$B = \frac{1}{2}\left[\exp(ikn_\varphi h) - \exp(ikn_\perp h)\right]\sin 2\psi$, $\quad k = 2\pi/\lambda -$ wave vector.

As to the condition $\varphi = \text{const}$, let us note that it is only approximate one and it is valid only for $h/\Lambda << 1$. At $h/\Lambda \approx 1$, the intensity of the electric field changes significantly along the FLC thickness. As the illustration, Fig.18 gives the plots of E_z component of electric field in the isotropic space between two electrodes, the potential at one of which being changing harmonically: $U(x) = U_O\left[1 + p\cos\left(2\pi\frac{x}{\Lambda}\right)\right]$, $\quad p < 1$.

For definiteness sake, let us assume that the vector of grating is parallel to X-axis (under approximation taken, DE is independent on the vector of grating orientation). Than the diffraction efficiency DE_p for linear-polarized reading light, with the polarization at the angle β to smectic layers, and the diffraction efficiency DE_{np} for non-polarized light can be expressed as:

$$\begin{aligned} DE_p &= |A_1|^2\cos^2\beta + |C_1|^2\sin^2\beta + \mathrm{Re}\left[(A_1 + C_1)B_1^*\right]\sin 2\beta + |B_1|^2, \\ DE_{np} &= \frac{1}{2}\left(|A_1|^2 + |C_1|^2\right) + |B_1|^2, \end{aligned} \tag{4}$$

here (*) is the complex conjugation sign, $A_1(B_1, C_1) = \frac{1}{\Lambda}\int_0^\Lambda A(B,C)\exp\left(-2\pi i\frac{x}{\Lambda}\right)dx$.

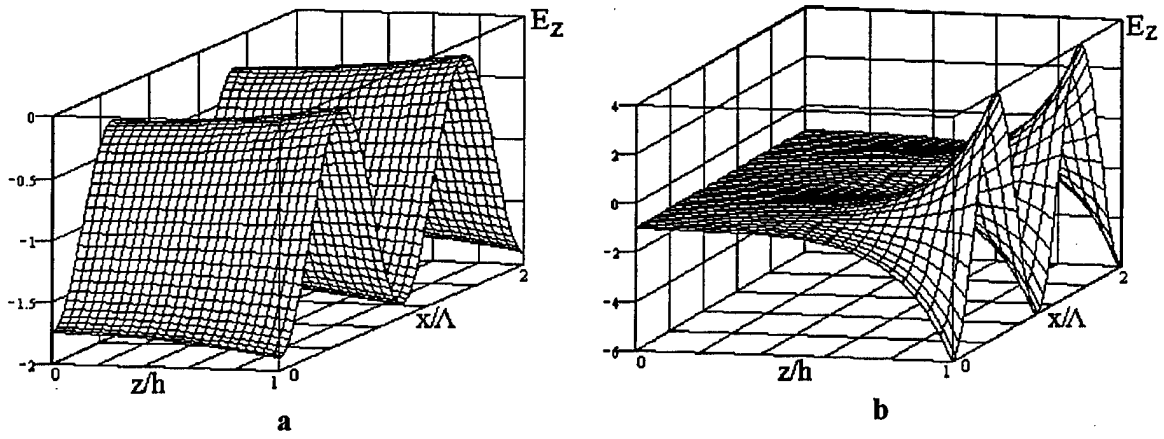

Fig.18. Spatial distribution of E_z component of the intensity of electric field at p = 0.8, h/Λ = 0.1 (a), 1 (b).

Let us apply these expressions for the analysis of DE behavior of diffraction gratings written using Clark-Lagerwall and DHF effects.

5.2. Clark-Lagerwall effect

The effect of Clark-Lagerwall manifests itself in re-orientation of the director n from one into another stable state under the change of sign of electric field E [5]. The azimuthal angle φ may get one of two values, 0 or π. Let us consider the case when the grating is being written with the Π-shape groove profile, and when the voltage at non-exposed zones of photoconductor is so small that FLC does not switch from one stable state into another. Than the change of the angle φ will be described as:

$$\varphi(x) = \begin{cases} 0, & 0 \le x < p\Lambda, \\ \pi, & p\Lambda \le x < \Lambda. \end{cases}, \quad p < 1 \tag{5}$$

Using expressions (1-5) it is easy to see that DE is independent of the direction of the polarization of the reading light, and it can be determined as:

$$DE_p = DE_{np} = \frac{4}{\pi^2}\sin^2(p\pi)\sin^2(2\theta)\sin^2\left(\frac{\Gamma}{2}\right), \tag{6}$$

here $\Gamma = k(n_{\parallel} - n_{\perp})h$ is the phase retardation. This formula gives the maximum for DE at p = 1/2, θ = π/4 and $\Gamma = (2m + 1)\pi$, = 0,1,2...

The conclusion on the DE independence of the polarization direction is in evident contradiction with experimental data (SLM D2). In our reasoning, this independence is the result of assumption of the absence of FLC switch inside the non-exposed zones. In order to determine the real situation, auxiliary experiments have been performed. Special LC cell was prepared, with the thickness h = 4μm, and was filled with the same LC as the SLM D2. The LC cell response was studied, the cell being placed between crossed polarizers, under illumination by CW light of He-Ne laser, probing light polarization direction being parallel to the normal to smectic layers. The cell was driven by Π-shape electric pulses with V_{pp} = 20 V with the voltage V_b varied. In the accordance with the known formula [5], the transmission of the cell must obey the $\sin^2(2\psi)$ law. Our experiments have shown that, even under very small values of the difference ($V_{pp} - V_b$) equal to tenths of volt, the switch of FLC occurs from the initial stable state into the state with φ = π/2 (and ψ = 0, correspondingly). Then the relaxation takes place into the another stable state, with the characteristic time dependent on difference

($V_{pp} - V_b$). This time can be several hundred milliseconds (see Fig. 19). The oscillograms were taken at the driving voltage repetition rate F = 10 Hz.

These experiments evident that the variations of the angle φ take place not between {0, -π}, but between {0 - π/2}. Assigning the function φ(x) as

$$\varphi(x) = \begin{cases} 0, & 0 \le x < p\Lambda, \\ \pi/2, & p\Lambda \le x < \Lambda. \end{cases}, \quad p < 1 \tag{7}$$

It is easy to get the following expressions for DE value:

$$DE_p = \frac{4}{\pi^2}\left[\left(\left\{\sin^2\frac{\hat{\Gamma}}{2} - \sin^2\frac{\Gamma}{2}\right\}\sin^2\theta + \sin^2\frac{\Gamma-\hat{\Gamma}}{2}\cos^2\theta\right)\cos^2\beta + \frac{1}{2}\sin\frac{\Gamma}{2}\cos\frac{\hat{\Gamma}}{2}\sin\frac{\Gamma-\hat{\Gamma}}{2}\sin 2\theta \sin 2\beta + \sin^2\frac{\Gamma}{2}\sin^2\theta\right]\sin^2 p\pi,$$

$$DE_{np} = \frac{2}{\pi^2}\left[\left(\sin^2\frac{\Gamma}{2} + \sin^2\frac{\hat{\Gamma}}{2}\right)\sin^2\theta + \sin^2\frac{\Gamma-\hat{\Gamma}}{2}\cos^2\theta\right]\sin^2 p\pi, \tag{8}$$

where $\hat{\Gamma} = \frac{g\Gamma}{1-g}\left[\left(\sin^2\theta + g^2\cos^2\theta\right)^{-1/2} - 1\right]$.

The Fig. 20 gives the result of DE calculation for g = 0.91, p = 1/2, and for three values of the angle θ. The DE values are normalized to the value $4/\pi^2$ representing the maximal DE value for the grating with Π-shaped grooves. The plots on the Fig.20b are given for the phase retardation Γ bringing the maximum for DE_n.

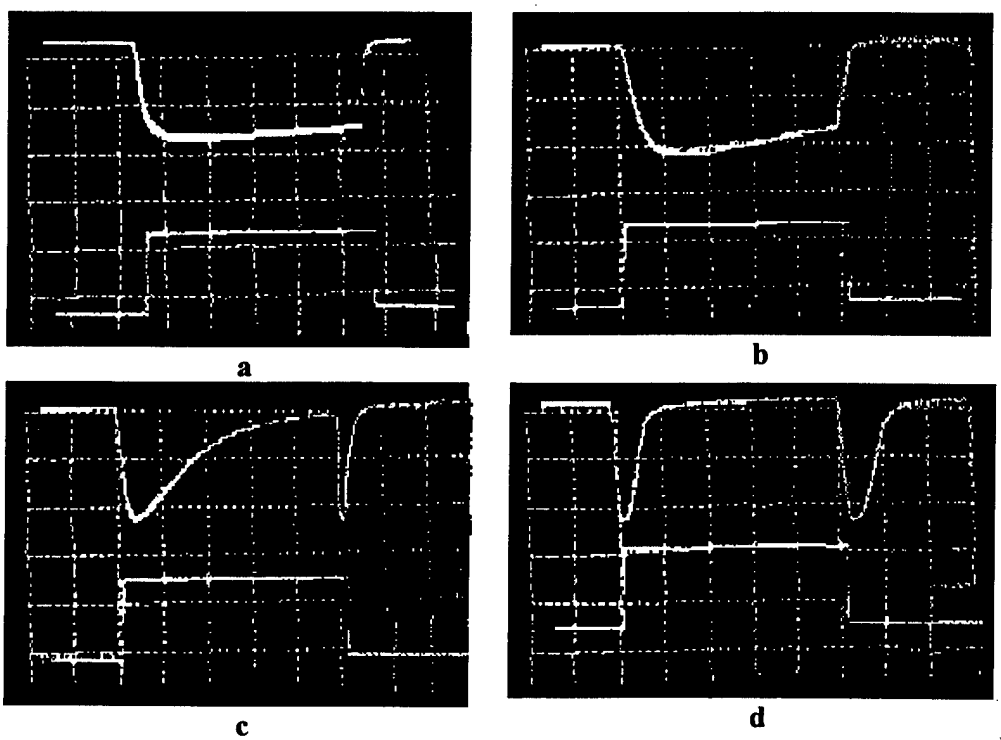

Fig.19. Oscillograms illustrating the dynamics of FLC re-orientation. Driving voltage (V_{pp} - V_b) = 0.5 (a), 1 (b), 2 (c) and 11 (d) volts; 1 division = 10 ms.

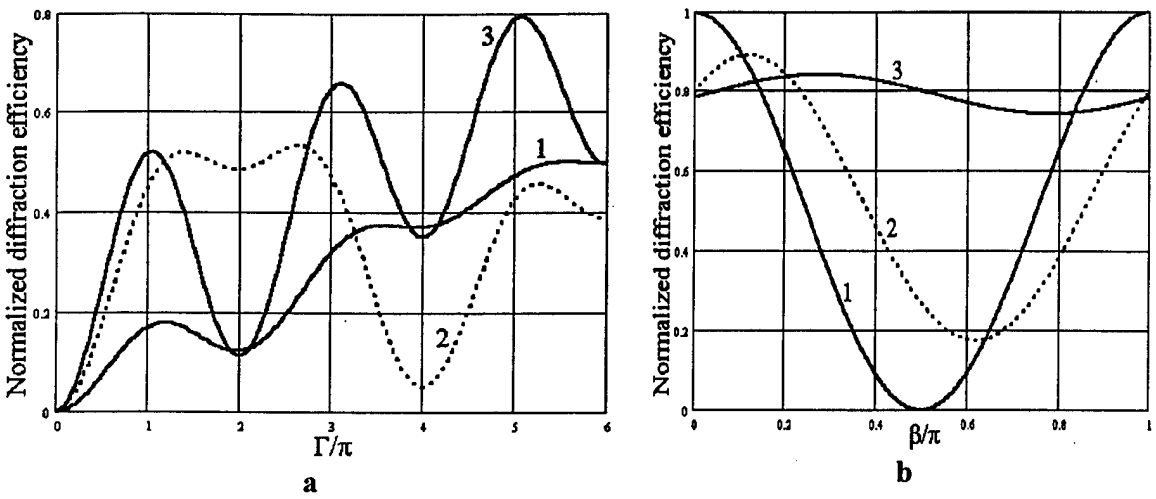

Fig.20. The normalized functions DE_{np} vs phase retardation (a) and DE_p vs direction of polarization of reading radiation (b) for $\theta = 22.5$ (1), 40 (2) and 65 (3) degrees.

The curves 1 and 2 in the Fig.20b are very similar, qualitatively, to the experimental curves for SLM D2, Fig.14. We see here, as well, the significant difference in DE values for the cases of reading light polarization parallel and perpendicular to the normal to smectic layers. Also, the maximal DE value is obtained far from always for the angle $\beta = 0$. It may be concluded from the expressions (8) that, under reading with linear-polarized light, the maximal limiting value of DE_p can be reached for the certain direction of polarization and for the certain values for Γ, θ and g (e.g., $\beta = 0$, $\Gamma = 6\pi$, $\theta \approx 22.5$ deg, and $g = 0.91$). At the same time, this maximal value DE_{np} will be only equal to 0.5 of the limiting DE value (as well as for NLC). In order to realize higher DE_{np} values, a certain phase retardation must be chosen, together with an angle θ. It is evident form (8) that the DE_{np} grows together with the angle θ, reaching its maximum at $\theta \approx 65$ deg. At the present, however, FLC with the molecule tilt angle exceeding 45 deg. are not known.

5.3. DHF-effect

The DHF effect essence is as follows. At the thermodynamically-equilibrium state, under the absence of electric field, the FLC director makes a spiral with the equilibrium pitch $p_0 << h$ turning on the generatrix of the cone as the coordinate along the helicoidal axis changes. Under the electrical field applied, the spiral rotation of FLC is being deformed, and the birefringence occurs. The effect exists until the full spiral unbending. This takes place when the modulus of electric field exceeds a critical value E_c [5].

The geometry of DHF effect and the deformation of the spiral are shown on Fig.21 and 22. The deformation of spiral is being calculated using the following relations [7]:

$$x(\varphi) = \frac{p_0}{2\pi}\int_0^{\varphi}\left[C + R\left(\frac{E}{E_0}\cos\phi + 1\right)^2\right]^{-1/2} d\phi, \quad \int_0^{\pi}\left[C + R\left(\frac{E}{E_0}\cos\phi + 1\right)^2\right]^{1/2} d\phi = \pi, \qquad (9)$$

where $E_0 = P_C / 2\varepsilon_0\varepsilon_a$, $R = P_C^2 p_0^2 / 8\pi^2\varepsilon_0\varepsilon_a K_e$, $\varepsilon_a = (\varepsilon_{||} - \varepsilon_{\perp})\sin^2\theta$,

$\varepsilon_{||}$ and $\varepsilon_{\perp}$ are the longitudinal and transverse components of dielectric permeability, ε_o is the vacuum permeability, K_e is the elasticity modulus. At $E = 0$, as it easy to see, $\varphi(x) = 2\pi x/p_o$. As $|E/E_c|$ approaches to 1, the pitch of the spiral tends to infinity, and the angle φ acquires one of two values: 0 or π.

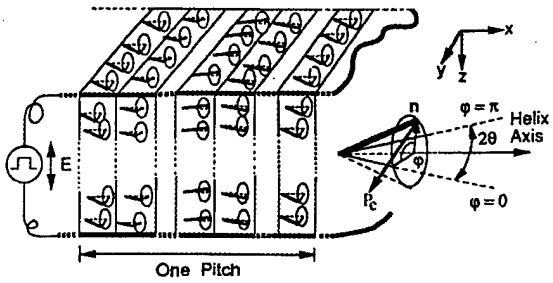

Fig.21. DHF effect geometry [6].

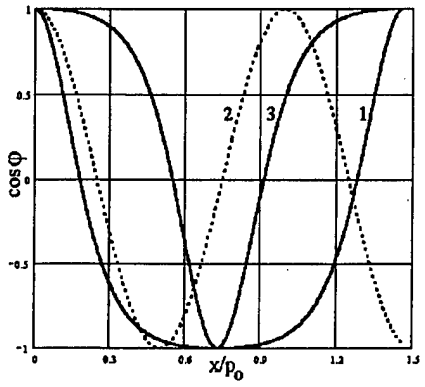

Fig.22. Variations of the azimuthal angle φ along the spiral axis at E/E_c = -0.95 (1), 0 (2), 0.95 (3) and R = -10.

To calculate DE with DHF effect, let us assume the following model of the diffraction grating formation. As it was above, the grating grooves profile is taken Π-shaped. For the exposed zones of PC, the intensity of electric field is assumed to be higher than the critical one for FLC, so the spiral is fully unbended (let us take, for definiteness sake, $\varphi = 0$, $\psi = \theta$). As for the non-exposed zones of PC, we admit the existence of such deformations of spiral that are arbitrary close to the another unbended state of spiral ($\varphi = \pi$, $\psi = -\theta$). As the background to this assumption, let us note that during the erasing stage of the working cycle the electric field is applied to FLC with intensity higher than the critical value. As the result, under change the E sign and for $|E/E_c| << 1$, the dependence of the birefringence of the voltage E applied has the expressed hysteresis character [5,8]. The relaxation time from the unbended state ($\varphi = \pi$) into the state characteristics for the voltage E, may be very long [5]. Let us assume, for DE calculation, that the deformation of the spiral is the same as the deformation in static field under a certain effective field intensity, with $|E_{eff}/E_c| < 1$. So, the change of the angle φ is described by the following function:

$$\varphi(x) = \begin{cases} 0, & 0 \le x < p\Lambda, \\ f(x), & p\Lambda \le x < \Lambda, \end{cases} \quad p < 1, \tag{10}$$

here $f(x) = f(x+P_E)$ is a periodic function determined from (9) at $E = E_{eff}$, with P_E being the pitch of the deformed spiral.

It was taken under calculations of coefficients A_1, B_1 and C_1 in formulae (4) that $P_E << \Lambda$. This condition is well fulfilled for the FLC, used in SLM D3 ($|R| >> 1$, Pc ~ 150-200 nK/cm^2 and $p_o \approx 0.2$ μm). Indeed, for $|E_{eff}/E_c|$=0.999 the pitch of the deformed spiral is only $2.3p_o$, as evaluated using the formula (9). As it was before, the DE values, under the condition of small spiral pitch, are proportional to $\sin^2 p\pi$.

The results of calculations of diffraction efficiency DE_p and DE_{np} are presented on Fig.23. The calculations are made at g = 0.91, p = 1/2, R = -10, angle θ = 40 deg, and fir several values E_{eff}. The plots in Fig.23b are given for the values of the phase retardation Γ that deliver the maximum for DE_{np}. It is evident from the plots that the weak polarization dependence of DE_p and the relatively high values of DE_{np} are realized when the helicoidal spiral is sufficiently unbended in the non-exposed zones of PC, and the phase retardation has a definite value close to the one of values $\Gamma = (2m + 1)\pi$ (m = 0,1,2,...). The calculations show that the value of DE_{np} under the angle θ varied reaches its maximum at $\theta = \pi/4$. The maximal value of DE_{np} is about ~ 0.7 of the maximal value of DE for the grating with the Π-shaped groove under the

variation of its parameters g and R in wide ranges.

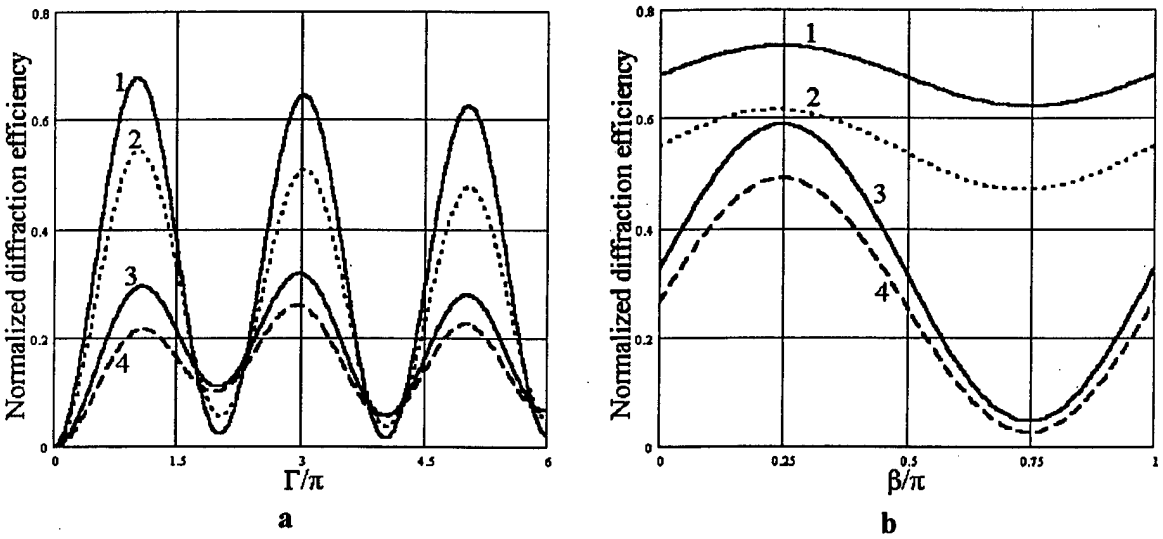

Fig.23. The normalized dependence of DE_{np} vs. phase retardation (a), and DE_p vs direction of the polarization of reading light (b) at E_{eff}/E_c = -0.999 (1), -0.95 (2), 0 (3) and 0.5 (4).

5.4. Conclusion

As the result of studies performed, it was discovered that the weak dependence of diffraction efficiency of hologram-correctors of the orientation of the reading light polarization, for the Clark-Lagerwall effect can be realized using FLC with the tilt angle of LC molecules about 65 deg. For the DHF-effect, this effect is not significant, provided that inside the non-exposed zoned of photoconductor the FLC spiral is unbended to the same state as it was during the erasing stage. At the same time, the maximal value of DE under reading by non-polarized light never reaches its limiting value but only about ~ 0.7 of this maximum. Notice that this conclusion of the maximal limiting value of DE_{np} is done basing on the model of holographic grating formation during the write-in stage. It is possible, in principle, such mode of OA SLM operation when the response appears during the erasing stage [9]. In this case, the diffraction grating in OA SLM is being formed due to difference in relaxation speed of LC molecules from one stable state into another. Of course, for this case the maximal limiting value of DE_{np} may be quite another.

6. Design and characteristics of developed OA SLM samples.

Basing on the results of studies performed, three samples of OA SLMs were manufactured. The design of OA SLM is shown in the Fig.24. The dielectric mirrors included 15 λ/4 layers of oxides HfO_2 and SiO_2. The DHF effect was chosen for refractive index modulation. The FLC tilt angle within the molecular layer was equal to 40 deg., $P_C \sim 150$ nK/cm^2 and $p_o \sim 0.2$ μm. The thickness of spacers was equal to 5 μm.

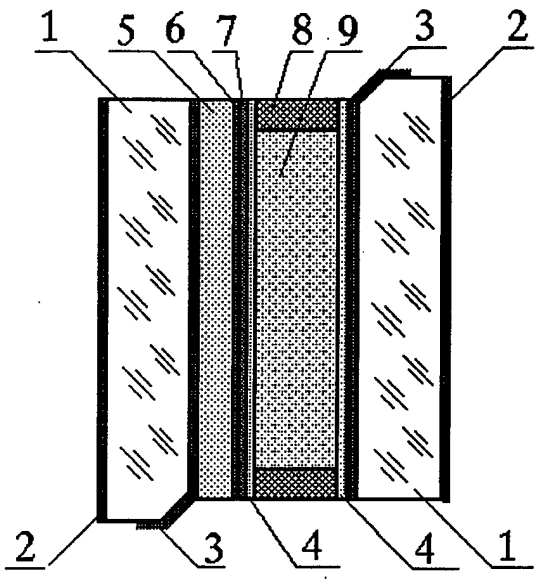

Fig.24. OA SLM design:

1. optical glass flat substrate,
2. antireflecting coating,
3. transparent electrodes,
4. alignment layers,
5. photoconductor,
6. opaque blocking layer,
7. dielectric mirror,
8. spacer,
9. ferroelectric liquid crystal.

The gratings were written using He-Ne laser, and the laser having the wavelength 0.53 μm was used for reading out. OA SLM feeding voltage: Π-shaped pulses with the duration 5 ms and repetition rate 100 Hz, with voltage $V_{pp} \approx 55$ V and bias voltage $V_b \approx -25$ V. The writing light beam intensity was modulated by Π-shaped pulsed with time duration 5 ms with the repetition rate 100 Hz. The maximal DE value was obtained when a delay ~3-4 ms was provided between OA SLM feeding and modulating pulses. When the gratings were written with the spatial frequency less than 25 lp/mm, the net optical efficiency was equal to 20-22% and it was practically independent on the direction of the reading light polarization. A significant decrease of DE was observed at the spatial frequency increase (see Fig.15).

7. Conclusion

The study showed that a flexible design FLC OA SLMs with using a-C:H LBL for optical decoupling between the write and read light beams is possible. We concluded that the a-C:H LBL 0.3-0.5 μm thick and with the resistivity lying within the 10^{10} -10^{11} Ωcm range and properly matches the FLC layer is suitable for optical isolating of the intrinsic a-Si:C:H photoconductor from green light. The results of our work make a promise the development of novel FLC OA SLMs operating in reflective mode. A careful optimization of the conductivity and the rise of reflectivity of dielectric mirror, as well as using the a-C:H LBL between the photoconductor and DM, will be required to achieve fast response, low-power operation, and the high spatial resolution of OA SLMs. Farther we plan to prepared the dielectric mirrors with improved optical and electrical properties.

The measurements of DE has revealed the significant influence of the write-in regime of holographic gratings to the dependence of DE on the blocking layer and mirrors characteristics. The studies show the importance of thorough matching of electrical impedance of dielectric mirrors, light blocking layers, and photoconductor in order to obtain the SLM characteristics specified for this work.

As a result of the works performed, samples of OA SLM are developed and manufactured containing dielectric mirrors and blocking layers. These samples have the net optical efficiency not less than 20% at the grating spatial frequency up to 25 lp/mm. This net optical efficiency can be realized for the repetition rate up to 100 Hz and it practically does not depend on the direction of the reading-out light polarization. For the grating spatial frequency increased up to 25-30 lp/mm, a significant decrease of DE is observed. This decrease is connected, mainly,

with the presence of dielectric mirror within SLM (transmissive OA SLMs using the same PC exhibit high DE values at much greater spatial frequency [9]). Probably, it is necessary, as minimum, to match electrical characteristics (conductivity and dielectric permeability) of mirror and FLC layer which is not a simple task. Seemingly, the success here may be reached with dielectric mirrors using a-Si:C:H layers instead of mirrors based on Hf and Si oxides.

References

1. E. A. Konshina, *Tech. Phys.*, to be published.
2. S. Egret, J. Robertson, W. I. Milne, and F. J. Clough, *D & RM*, Vol. 6, 879, 1997.
3. A. Grill, V. Patel, and S. Cohen, *D & RM*, Vol. 3, No. 3, 281, 1994.
4. D. I. Jones and A. D. Stewart, *Philos. Mag. B*, Vol. 46, No. 5, 423, 1982.
5. G. S. Chilaya, V. G. Chigrinov, , "Optical and electrooptical effects in chiral smectic C liquid crystals", Uspekhi Fizicheskih Nauk, Vol. 163, No. 10, pp. 1-28, 1993 (in Russian).
6. I. Abdulhalim, G. Moddel, "Electrically and optically controlled light modulation and color switching using helix distortion of ferroelectric liquid crystals," *Mol. Cryst. Liq. Cryst.*, Vol. 200, pp. 79-101, 1991.
7. V. E. Dmitrienko, V. A. Belyakov, "On the structure of chiral smectics in electric field", *Zh. Eksp. i Teor. Fiz.*, Vol. 78, No. 4, pp. 1568-1578, 1980 (in Russian).
8. L. A. Beresnev, L. M. Blinov, Д. I. Dergachev, M. V. Loseva, N. I. Chernova, "Electrooptic response of a thick layer of ferroelectric liquid crystal with small step of helicoide and high spontaneous polarization", *Pisma v ZhTF*, Vol. 14, No. 3, pp.260-263, 1988 (in Russian).
9. D. V. Wick, T. Martinez, M. V. Wood, J. M. Wilkes and M. T. Gruneisen, V. A. Berenberg, M. V. Vasil'ev, A. P. Onokhov, "Deformed-helix ferroelectric liquid-crystal spatial light modulator demonstrating high diffraction efficiency and 370 line pairs per millimeter resolution," *Appl. Opt.*, Vol. 38, No. 17, pp. 3798-3803, 1999.